Measurements of sea-floor backscattering strength of very low frequency acoustic waves in western Mediterranean Sea; a comparison to GABIM [1]

Iannis Bennaceur[1], Nathan Ivkovic[1], Xavier Cristol[1], Adrien Rondeau[1], and Benoit Theckes[1]

[1]Thales Defence Mission Systems, FRANCE

Iannis Bennaceur, 525 route des dolines, 06560 Valbonne, FRANCE
iannis.bennaceur@fr.thalesgroup.com, +33492963291

Abstract: *In the context of anti-submarine warfare, active sonar performances depend on the amount of reverberated energy reaching the receiver after the powerful emission from the source. In the Very Low Frequency (VLF) range, the scattering by the seafloor provides the largest contribution to the reverberation level that THALES DMS (TDMS) UWS tries to better predict. An at-sea trial took place in the Mediterranean Sea in September* 2024*,* 30 *km off French Riviera coast in a deep-water environment. Two boats were involved, one carrying an acoustic source emitting at* 215 *Hz, immersed at* 6.7 *m under the sea-surface, the other conveying a vertical line array composed of* 13 *hydrophones spaced by* 3 *m. The center of the antenna was* 45 *meter below the sea-surface. The boats were spaced from few dozen meters, and* 1*-second Continuous Waves (CW) were transmitted in order to measure the acoustic Reverberated Level (RL) in this quasi-monostatic configuration. The output of classical weighted beamforming according to time and elevation angle allowed to extract RL according to the grazing angle* θ *in a range between* 25 *and* $65°$*. The evolution of the backscattering strength* σ*, deduced from RL, regarding* θ *is in good agreement with other measures that also took place in the Mediterranean Sea [2] where two regimes were noticed; lower level of* σ *for* $\theta \leq 30°$ *issued from the scattering by the volume of sediments, and higher level for* $\theta \geq 35°$ *mainly issued from the scattering by the rough interface between the sediment and the harder basement. Finally, our implementation of GABIM [1] computed for several sediment thicknesses and volume backscattering strengths are compared to our measurements.*

Keywords: *Sea-floor reverberation, backscattering strength, very low frequency, GABIM*

1. ENVIRONMENT AND REVERBERATED LEVEL

During the trial (see abstract for details), the water temperature from the sea-surface to a depth of $750\,\mathrm{m}$ was measured using a Sippican probe. The resulting celerity profile, extended to the water height ($H_w \approx 2388\,\mathrm{m}$) and displayed on the left part of Fig. 1, exhibits a strong thermocline. To construct a geoacoustic model for the sea-floor (right part of Fig. 1), needed for the σ computation, the closest site of the Deep Sea Drilling Project relative to our measurements location is considered. At site 372 (east Menorca rise), a $150\,\mathrm{m}$ thick layer of marls from the Plio-Quaternary overlies late Miocene gypsum and dolomitic marls. We choose as superficial properties for those marls (or sandy muds), a porosity of 0.7, a compressional velocity ratio c_p/c_w, with c_w the water sound speed just above the sediment, of 1.013, and a compressional attenuation k_p in dB/m/Hz of 101.8. The evolution of celerity, attenuation and density ρ regarding depth up to $150\,\mathrm{m}$ are computed using Hamilton's work [3]. The celerity and density in the late Miocene layer (dots on Fig. 1), considered as a semi-infinite layer, comes from the CRUST1.0 model [4]. All the layers are considered fluid (no shear effect).

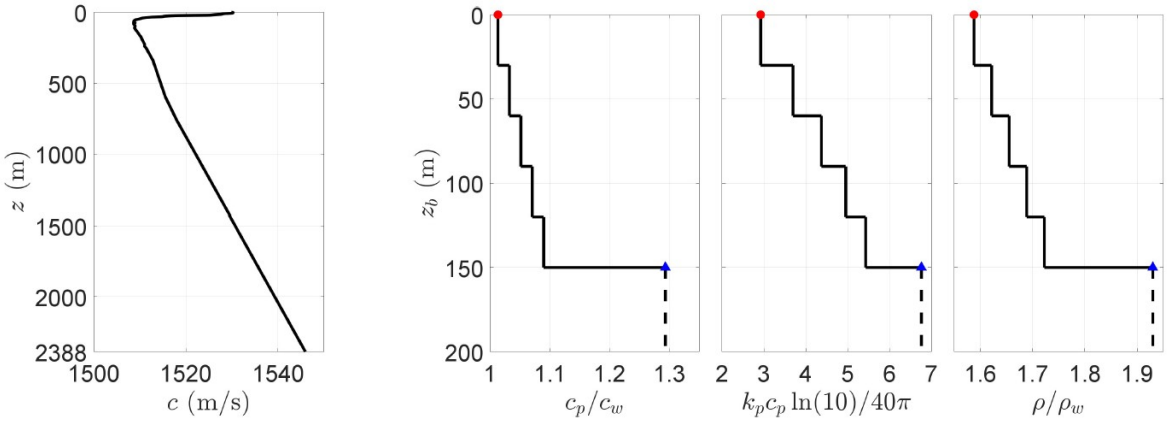

Figure 1: ***Left:*** *Sound-speed volcity profile in water,* ***right:*** *evolution regarding depth in the sediment layer of the compressional velocity ratio c_p/c_w, normalized compressional attenuation (k_p in dB/m/Hz), and density ratio ρ/ρ_w where $\rho_w = 1\,g/cm^3$.*

Weighted (Hann's window in time and Hamming's in space) overlapped ($50\,\%$) classical beamforming according to time and elevation angle ϕ is performed over the 20 1-s CW emissions. The rapid variation in time of the reverberated field direction of arrival requires short FFT. We choose to perform FFT over 1024 samples (a quarter of the sampling frequency) leading a frequency resolution of $4\,\mathrm{Hz}$. Hence, a 2D cubic interpolation in the (f, ϕ) domain for each temporal bloc is performed to measure the Reverberated Level RL in dB re $1\,\mu\mathrm{Pa}/\sqrt{\mathrm{Hz}}$ at $215\,\mathrm{Hz}$. Simulation indicates that this operation leads to a bias that do not exceed $+0.25\,\mathrm{dB}$. The 20 outputs of beamforming are then averaged and RL is extracted (white dots on Fig. 2).

2. GABIM IMPLEMENTATION

In the process of implementing GABIM [1], one needs to extract from OASR (one of the software included in the Ocean Acoustics and Seismic Exploration Synthesis (OASES) [5]) the up-going and down-going waves complex amplitudes, A and B respectively, in each layer. We

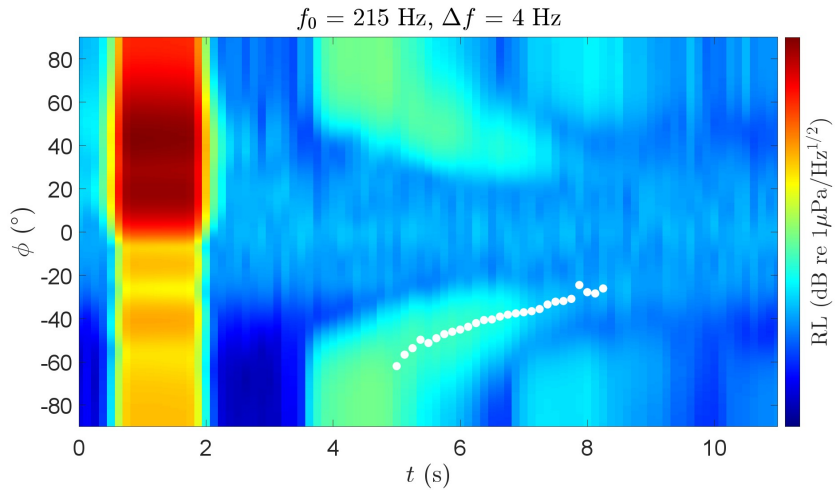

Figure 2: Averaged beamforming output on which the reverberated level is extracted (dots).

validate this process by successfully comparing our implementation to Fig. 5 of [1] on left part of Fig. 3 that represents the scattering from a very rough rock basement under a smooth sand layer. A second verification consisted in plotting Fig. 11 of [1] with the parameters given in the corrected addendum [6]. The right upper part of Fig. 3 shows strong, unexplained, oscillations for the water-sediment interface roughness and the volume contributions to backscattering strength. A way to reduce the oscillations regarding the water-sediment interface roughness is to consider Eq. (42) of [7] (valid when sediments velocity and density are homogeneous (no gradients)) instead of Eq. (32) of [1]. To reduce the volume contribution oscillations, we have split Eq. (43) of [1] into oscillating-terms proportional to BA^*, with $\cdot^*$ the complex conjugation, and non oscillating-terms proportional to $|A|$ and $|B|$, and only consider the latter for the scattering strength computation. The right lower part of Fig. 3 shows that the oscillations disappeared at the cost of a 5 dB discrepancy in the total scattering strength, for some θ range below 35°. Nevertheless, the overall agreement is reasonable and contacting the authors may help understanding the origins of these oscillations.

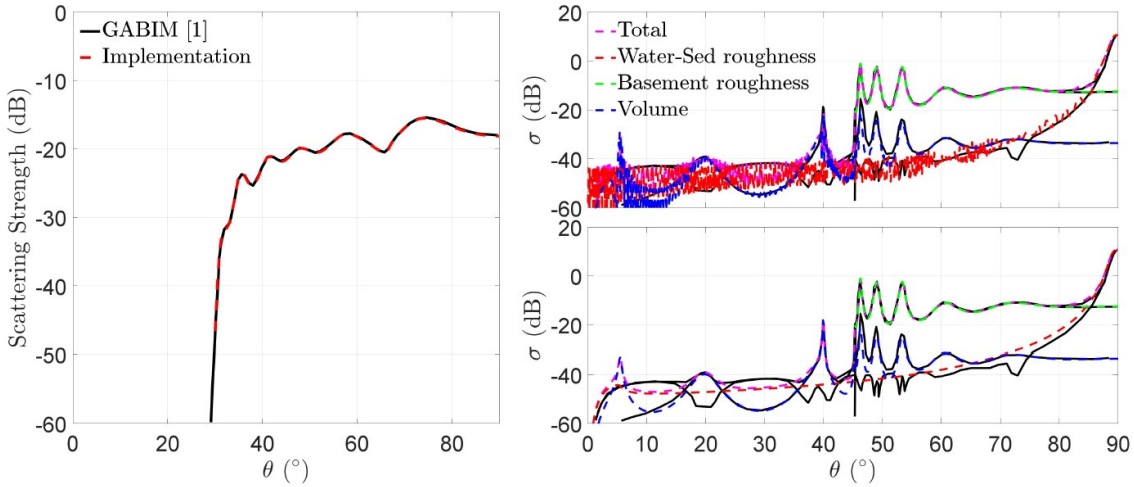

*Figure 3: **Left:** Fig. 5 of [1], **right:** Fig. 1 of [6], without (upper part) and with (lower part) oscillations corrections.*

3. BACKSCATTERING STRENGTH COMPUTATION

The backscattering strength σ in dB is computed following:

$$\sigma = \mathrm{RL} - \mathrm{SL} - 10\log_{10}\left(2\pi \int_{R_{\min}}^{R_{\max}} r\mathrm{d}r\mathrm{TL}_g(r)\mathrm{TL}_r(r)D_a(\phi(r),\theta_m(r))\right), \quad (1)$$

where RL is the reverberated level extracted from Fig. 2, SL the source level at 215 Hz in dB re $1\,\mu$Pa/$\sqrt{\text{Hz}}$ @1 m, TL_g and TL_r the transmission losses (re 1 m) from the source to the ensonified area and from the area to the antenna, respectively, and D_a the antenna directivity pattern. $R_{\min}$ and $R_{\max}$ correspond to the inferior and superior radial integration limits, computed numerically with a ray-tracing code, defined such that the go and return time travel $t_0(r)$ is in between $t - \tau/2$ and $t + \tau/2$ where t is the time of the RL measurement and $\tau = 1$ s the CW pulse duration. As the measure of RL at t is the sum of the contributions from all area elements in between $R_{\min}$ and $R_{\max}$, that have been ensonified under a grazing angle from $\theta_{\min}$ to $\theta_{\max}$, one choose to represent the evolution of σ according to a "mean" grazing angle defined as $\theta_m = 0.5(\theta_{\min} + \theta_{\max})$. In Eq. (1), the antenna directivity pattern is taken into account as followed: while pointing in the θ_m direction, the contribution of all area elements is weighted by the directivity pattern evaluated at the elevation angle of arrival ϕ on the antenna, different for each elements. The 2π factor indicates that we already performed the azimuthal integration allowed by the quasi-monostatic configuration of the trial. Finally, all the terms inside the integral in Eq. (1) are expressed on a linear scale.

As the source is immersed near the sea-surface (6.7 m) and the emitted wave-length is close (≈ 7.1 m), one needs to be careful when computing the incident pressure field (or TL_g in Eq. (1)) on the ensonified areas. In such configuration, the summation of the complex pressure field (intensity plus phase) associated with each ray should be favored. This produces an emission directivity pattern ("Llyod mirror") that has on strong influence on the incident pressure field at the sea-floor (see left image of Fig. 4). In contrast, the incoherent summation of intensity only produces a incident pressure field on the sea-floor that decays slowly with respect to r (right image of Fig. 4).

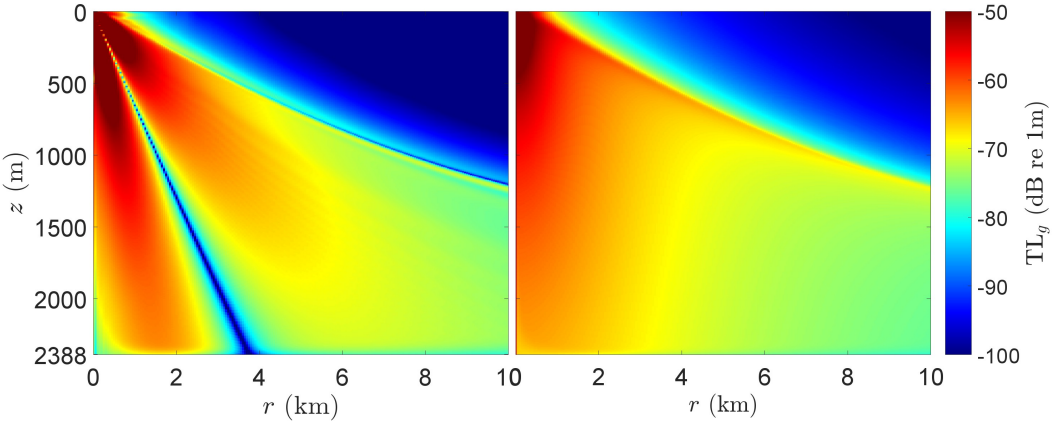

Figure 4: ***Left:*** *Coherent pressure field,* ***right:*** *incoherent pressure field.*

The computation of σ following Eq. (1) is realized with both $\mathrm{TL}_g^{(C)}$ and $\mathrm{TL}_g^{(I)}$, the transmission losses from the source to the sea-floor obtained from the coherent and incoherent summation, respectively. The scattering strengths are displayed, along with the measurements of [2],

against θ_m on Fig. 5 (left part). Using $\mathrm{TL}_g^{(C)}$ for the calculation of σ produces a strong bump for $\theta_m \approx 32° \approx \tan^{-1}(2388/3800)$ due to the zero in the emission directivity pattern, whereas σ based on $\mathrm{TL}_g^{(I)}$ is in a better qualitative agreement with past observations. One possible explanation is that the interaction between the acoustic wave and the 18-meters long boat that carries the source partially fills the zero of the directivity pattern. Regarding σ based on $\mathrm{TL}_g^{(I)}$, if the SL was not high enough to address the grazing angles lower than 25°, a strong decrease appears from $\theta_m \approx 33°$ suggesting a change in the scattering mechanism. The right part of Fig. 5 represents the three contributions to the total scattering strength issued from our implementation of GABIM calculated with the geoacoustic model described by Fig. 1 and the interpolation of the parameters σ_2 and w_2 found in Table I of [1] with respect to $a_\rho = \rho/\rho_w$. The parameters σ_2 and w_2 are the dimensionless volume backscattering cross section and the spectral strength of interface roughness, respectively. One sees that the contribution to σ of the water-sediment interface is negligible compared to the volume, and to the basement interface ones. The latter starts to contribute around 30°, once the incident grazing angle is large enough for the acoustic field to cross the sediments up to the late Miocene layer.

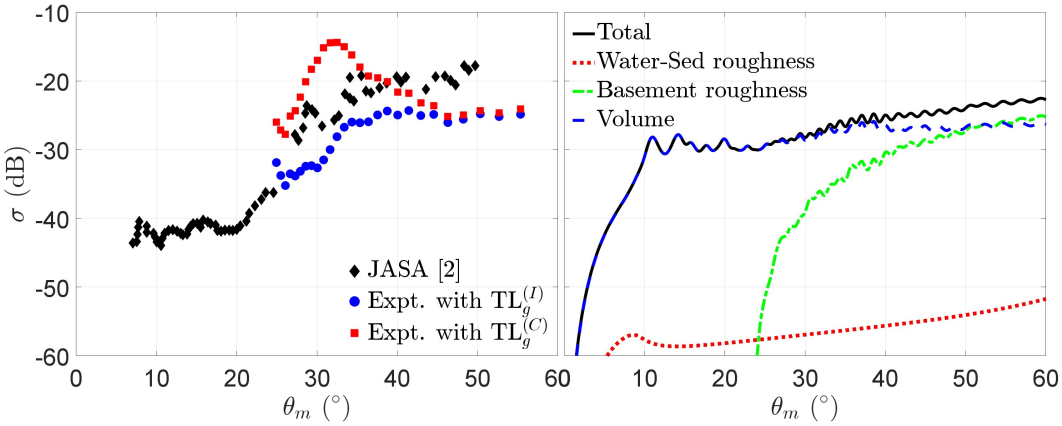

Figure 5: ***Left:*** *Measured backscattering strengths,* ***right:*** *detailed scattering contributions issued from our implementation of GABIM.*

The sensitivity of σ issued from our implementation of GABIM, regarding σ_2 and the sediments thickness h_s is displayed on Fig. 6, along with the measured scattering strength (based on $\mathrm{TL}_g^{(I)}$). Reducing by a factor of 4 the values of σ_2^G proposed by [1] (still remaining in the typical range from 10^{-4} to 5.10^{-2}) and reducing h_s from 150 to 125 m provides the best fit for σ. The significant variation of the modeled σ regarding σ_2 and h_s shows that a good agreement between measures and modeling requires a rightful geoacoustic model and a judicious choice for the parameters describing random variations. Nevertheless, the decent agreement obtained on Fig. 5 between measures and modeling based on a first-guess geoacoustic model (Fig. 1) and on the typical values given by Table I of [1] make us confident about using our implementation of GABIM for estimating reverberation level for very low frequency active sonar performances.

4. CONCLUSION

In this paper, a bottom backscattering strength measurement on a 1-s CW at 215 Hz in the western Mediterranean Sea is described. The acoustic source (immersed at 6.7 m) being in the

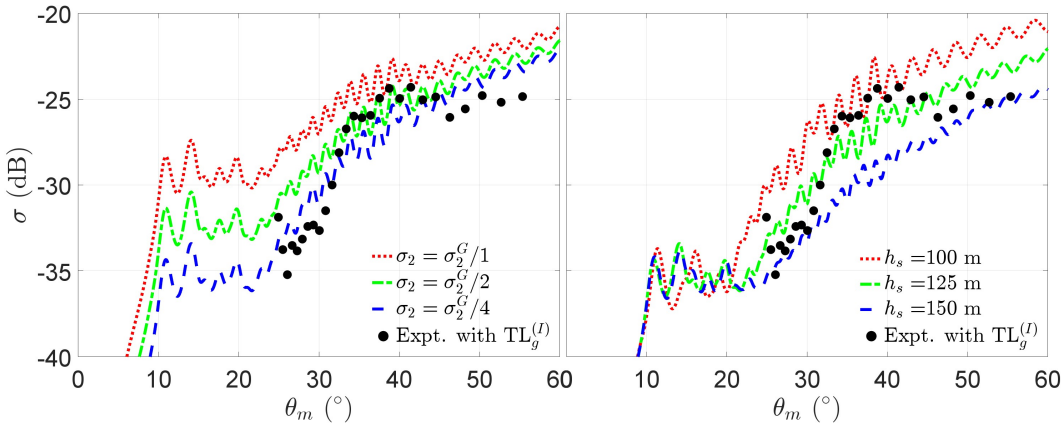

Figure 6: Scattering strength issued from our implementation of GABIM for ***left:*** $h_s = 125\,m$ *and several values of* σ_2, ***right:*** $\sigma_2 = \sigma_2^G/4$ *and several values of* h_s.

vicinity of the sea-surface, coherent and incoherent incident pressure fields may be considered for the measure of σ. While the zero in the emission beam pattern ("Llyod mirror effect") of the coherent field induces a strong bump in the backscattering strength, the computation of σ upon the incoherent field is in good qualitative agreement with past measurement. Two scattering mechanisms are suggested: lower level of σ for $\theta \leq 30°$ issued from the scattering by the volume of sediments, and higher level for $\theta \geq 33°$ mainly issued from the scattering by the rough interface between the sediment and the harder basement. Our implementation of GABIM [1], used with a first-guess geoacoustic model and the default parameters describing random variations provided in [1], exhibits both regimes and allowed decent agreement with the measurements.

REFERENCES

[1] D. R. Jackson, R. I. Odom, M. I. Boyd, A. N. Ivakin : "A Geoacoustic Bottom Interaction Model (GABIM)", *IEEE J. Oceanic Eng.* **35**, 603-617, **(2010)**.

[2] C. W. Holland, P. Neumann : "Sub-bottom scattering: A modeling approach", *J. Acoust. Soc. Am.* **104**, 1363-1373, **(1998)**.

[3] E. L. Hamilton, : "Geoacoustic modeling of the sea floor", *J. Acoust. Soc. Am.* **68**, 1313-1340, **(1980)**.

[4] G. Laske, G. Masters, Z. Ma, M. Pasyanos : "Update on CRUST1.0 - A 1-degree Global Model of Earth's Crust", *Geophys. Res. Abstracts* **15**, Abstract EGU2013-2658, **(2013)**.

[5] H. Schmidt : "OASES, Version 3.1, User Guide and Reference Manuel", *M.I.T, Cambridge* Tech. Rep., **(2004)**.

[6] D. R. Jackson, R. I. Odom, M. I. Boyd, A. N. Ivakin : "Corrections to "A Geoacoustic Bottom Interaction Model (GABIM)"", *IEEE J. Oceanic Eng.* **36**, 373, **(2011)**.

[7] J. E. Moe, D. R. Jackson : "First-order perturbation solution for rough surface scattering cross section including the effects of gradients", *J. Acoust. Soc. Am.* **96**, 1748-1754, **(1994)**.